

Transmission coefficient through a saddle-point electrostatic potential for graphene in the quantum Hall regime

Martina Flöser and Serge Florens

*Institut Néel, CNRS and Université Joseph Fourier, B.P. 166,
25 Avenue des Martyrs, 38042 Grenoble Cedex 9, France*

Thierry Champel

*Laboratoire de Physique et Modélisation des Milieux Condensés,
CNRS and Université Joseph Fourier, B.P. 166,
25 Avenue des Martyrs, 38042 Grenoble Cedex 9, France*

(Dated: February 23, 2024)

From the scattering of semicoherent-state wave packets at high magnetic field, we derive analytically the transmission coefficient of electrons in graphene in the quantum Hall regime through a smooth constriction described by a quadratic saddle-point electrostatic potential. We find anomalous half-quantized conductance steps that are rounded by a backscattering amplitude related to the curvature of the potential. Furthermore, the conductance in graphene breaks particle-hole symmetry in cases where the saddle-point potential is itself asymmetric in space. These results have implications both for the interpretation of split-gate transport experiments, and for the derivation of quantum percolation models for graphene.

PACS numbers: 73.43.Jn, 73.43.Cd, 71.70.Di, 73.22.Pr

The quantum point-contact geometry formed by metallic split gates in the quantum Hall regime is a cornerstone of many experiments in two-dimensional electron gases (2DEGs) based on semiconducting heterostructures. For example, in recent interferometry experiments made with electrons, the quantum point contact plays the role of an electronic beam splitter.¹ At the theoretical side, the consideration of a smooth constriction represents a simple toy model of elaborated quantum transport theories. For instance, the transmission coefficient through a saddle-point potential² is a central piece of the percolation network models,^{3,4} which have been introduced to describe the inter-plateaus dissipative transport in the quantum Hall effect.

Smooth constrictions are usually modeled by the local potential profile at the bottleneck of the constriction

$$V(\mathbf{r}) = by^2 - ax^2, \quad (1)$$

where a and b are real positive coefficients characterizing the potential (for convenience, we chose the electrostatic potential value at the saddle as the origin for the energies). Important insights on the tunneling processes determining the transport properties through quantum point contacts can be gained from the quantum mechanical motion of the electron in such a simple potential as given by Eq. (1). In the standard 2DEGs usually described by Schrödinger's equation, the energy dependence of the transmission coefficient through the quadratic potential in Eq. (1) is well-known and given under high magnetic fields (i.e., neglecting Landau-level mixing while keeping the magnetic length l_B finite) by the expression⁵

$$T_n(E) = \left[1 + \exp \left(-\pi \frac{E - \{n + 1/2\}(\hbar\omega_c + \zeta)}{l_B^2 \sqrt{ab}} \right) \right]^{-1} \quad (2)$$

for the n th Landau level, where $l_B = \sqrt{\hbar c/(|e|B)}$ is the magnetic length, $\hbar\omega_c$ is the Landau-level spacing in the 2DEG, and $\zeta = l_B^2(b - a)$. Tunneling processes give rise to a nonzero probability for the electron at energy $E < 0$ to be transmitted on the other side of the constriction while an electron at $E > 0$ goes weakly backscattered through the available channels.

With monolayer graphene consisting of carbon atoms packed in a two-dimensional honeycomb lattice appears a new host material,⁶ where electrons are confined to two dimensions, yet with some exotic properties. The observation of an anomalous quantum Hall effect in graphene^{7,8} understood in terms of a relativistic-like spectrum of low-energy electrons⁹ has been followed by numerous experimental and theoretical contributions¹⁰ aiming at exhibiting specific signatures of the 2D massless Dirac fermions in a non-uniform potential. The studies of simple analytical problems, such as the quantum-mechanical motion of massless particles in the quadratic saddle-point potential [(1)], are of valuable interest for identifying such unusual properties. However, it turns out that quadratic potentials, which are exactly solvable in ordinary 2DEGs at any magnetic field, become generally not analytically solvable within the Dirac equation. Here, we consider the regime of large magnetic fields, in which the Landau level spacing in graphene is large enough so that one can work in the single Landau-level limit. We have recently shown¹¹ using a semicoherent-state Green's-function formalism that quadratic problems then become soluble in this regime.

The determination of the transmission coefficient through a smooth constriction for graphene in the high magnetic field limit [i.e., the counterpart of Eq. (2)] is the main result of this Rapid Communication, that we start by discussing in relation to conductance quantization in

graphene, with a detailed derivation using semicoherent-state Green's functions making the rest of the Rapid Communication. The exact transmission coefficient for graphene in the absence of Landau-level mixing reads in the n th Landau level (with $n \geq 1$)

$$T_{n,\epsilon}(E) = \left[1 + \exp \left(-\epsilon\pi \frac{E - E_{n,\epsilon}}{l_B^2 \sqrt{ab}} \right) \right]^{-1}, \quad (3)$$

where $\epsilon = \pm 1$ is a band index characterizing the electron and hole-like contributions, and

$$E_{n,\epsilon} = n\zeta + \epsilon \sqrt{n(\hbar\Omega_c)^2 + \zeta^2/4} \quad (4)$$

with $\Omega_c = \sqrt{2}v_F/l_B$ (v_F is the graphene Fermi velocity). The transmission probability for the lowest Landau level ($n = 0$) is given by $T_0(E) = 1/2$.

The zero-temperature conductance at chemical potential μ is given in terms of the transmission probabilities by the Landauer-Büttiker formula

$$\mathcal{G}(\mu) = \frac{4e^2}{h} \left[T_0(\mu) + \sum_{n=1}^{\infty} \sum_{\epsilon=\pm} T_{n,\epsilon}(\mu) \right], \quad (5)$$

where we have accounted for the spin and valley degeneracies in graphene with the overall prefactor 4.

Then, as found in Ref. 12 for the 2DEG case, the conductance quantization in the graphene case shown in Fig. 1 directly follows from the transmission probabilities. The first obvious observation is the half-integer quantization of the conductance in terms of the conductance quantum (here $4e^2/h$) with plateaus at values $(n + 1/2)4e^2/h$, reminiscent of the half-integer quantization of the Hall conductance. Two different configurations, symmetric and asymmetric with respect to $\pi/2$ rotation of the saddle-point potential in Eq. (1), have been considered, which yield to two different curves. A symmetric saddle-point potential is characterized by $a = b$, thus $\zeta = 0$, and the conductance shows clear particle-hole symmetry with respect to change in the energy sign. In the case of an asymmetric saddle-point potential ($a \neq b$), ζ becomes non-zero, signaling a breaking of particle-hole symmetry in the energy levels Eq. (4), and resulting in a non-uniform shift of the conductance steps, which is more pronounced for the highest Landau levels. It is worth noting that the asymmetry of the potential in Eq. (1) has a different consequence in the case of the standard 2DEG, where it just leads to a redefinition of the Landau-level spacing, see Eq. (2), and such a small quantitative modification appears difficult to perceive in an experiment. In graphene, the effect of the potential asymmetry should be more easily seen in experiments, since it yields an asymmetry between the positive- and negative- energy dependences of the conductance.

Now, we focus on the derivation of Eq. (3). We consider a single-particle Hamiltonian model for an electron of charge $e = -|e|$ and of Fermi velocity v_F confined to

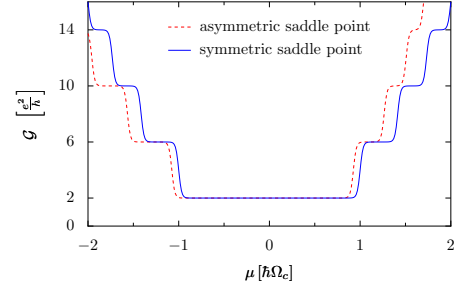


FIG. 1: (Color online) Zero-temperature conductance for a saddle-point electrostatic potential with $l_B^2 a = l_B^2 b = 0.05\Omega_c$ (symmetric case) and $l_B^2 a = 4l_B^2 b = 0.1\Omega_c$ (asymmetric case). Asymmetries of the electrostatic saddle-point potential reflect in asymmetries between the electron and hole sectors for the conductance.

a two-dimensional graphene sheet in the plane (x, y) in the presence of both a perpendicular uniform magnetic field $\mathbf{B} = B\hat{\mathbf{z}}$ and an electrostatic (scalar) potential term $V(\mathbf{r})$ [given by Eq. (1)]

$$\hat{H} = v_F \begin{pmatrix} 0 & \Pi_x - i\Pi_y \\ \Pi_x + i\Pi_y & 0 \end{pmatrix} + V(\mathbf{r})\hat{1} \quad (6)$$

with $\boldsymbol{\Pi} = -i\hbar\nabla_{\mathbf{r}} - e\mathbf{A}(\mathbf{r})/c$, where $\mathbf{A}(\mathbf{r})$ is the vector potential defined by the equation $\nabla_{\mathbf{r}} \times \mathbf{A}(\mathbf{r}) = \mathbf{B}$. Here $\hat{1}$ corresponds to the unity matrix in the pseudo-spin space (representing electron and hole degrees of freedom) and c is the speed of light. For convenience, we will omit both physical spin and valley indices, thus assuming that the two valleys of graphene remain completely decoupled from each other and can be studied separately. In addition, we shall not consider the effects of ripples or a mass potential but these could be studied following Ref. 11.

To describe the electron dynamics at high magnetic field, it is useful¹¹ to introduce the graphene vortex states

$$\tilde{\Psi}_{n,\mathbf{R},\lambda}(\mathbf{r}) = \frac{1}{\sqrt{1+|\lambda|}} \begin{pmatrix} \lambda\Psi_{n-1,\mathbf{R}}(\mathbf{r}) \\ i\Psi_{n,\mathbf{R}}(\mathbf{r}) \end{pmatrix}, \quad (7)$$

$$\Psi_{n,\mathbf{R}}(\mathbf{r}) = \frac{e^{-(|z|^2+|Z|^2-2ZZ^*)/(4l_B^2)}}{\sqrt{2\pi l_B^2 n!}} \left(\frac{z-Z}{\sqrt{2}l_B} \right)^n \quad (8)$$

with $z = x + iy$ and $Z = X + iY$. Here $\mathbf{R} = (X, Y)$ is a doubly continuous quantum number corresponding to the guiding center position in the plane, n is a positive integer, λ is a band index (defined for a given n), which is equal to ± 1 if $n \geq 1$, and 0 for $n = 0$. States in Eq. (7), which can be written as $\tilde{\Psi}_{n,\mathbf{R},\lambda}(\mathbf{r}) = \langle \mathbf{r} | n, \mathbf{R}, \lambda \rangle$ within the Dirac bracket notation, are eigenstates of Hamiltonian (6) in absence of the electrostatic potential ($V = 0$) with the energy quantization $E_{n,\lambda} = \lambda\sqrt{n}\hbar\Omega_c$. Despite being nonorthogonal with respect to the degeneracy quantum number \mathbf{R}

$$\langle n_1, \mathbf{R}_1, \lambda_1 | n_2, \mathbf{R}_2, \lambda_2 \rangle = \delta_{n_1, n_2} \langle \mathbf{R}_1 | \mathbf{R}_2 \rangle \delta_{\lambda_1, \lambda_2}, \quad (9)$$

$$\langle \mathbf{R}_1 | \mathbf{R}_2 \rangle = \exp \left[-\frac{(\mathbf{R}_1 - \mathbf{R}_2)^2 - 2i\hat{\mathbf{z}} \cdot (\mathbf{R}_1 \times \mathbf{R}_2)}{4l_B^2} \right] \langle 10 \rangle$$

the set of quantum numbers $|n, \mathbf{R}, \lambda\rangle$ obeys a completeness relation

$$\int \frac{d^2\mathbf{R}}{2\pi l_B^2} \sum_{n=0}^{+\infty} \sum_{\lambda} |n, \mathbf{R}, \lambda\rangle \langle n, \mathbf{R}, \lambda| = \hat{1}. \quad (11)$$

In fact, the states in Eq. (7) form an overcomplete basis of states, which have the *coherent states character* with respect to the quantum number \mathbf{R} .

Relation (11) allows one to project the electron dynamics onto the vortex representation. We can then introduce the vortex Green's function $G(n_1, \mathbf{R}_1, \lambda_1, t_1; n_2, \mathbf{R}_2, \lambda_2, t_2)$, which gives the probability amplitude for a vortex with circulation (or Landau-level index) n_1 and band index λ_1 that is initially at position \mathbf{R}_1 at time t_1 to be at point \mathbf{R}_2 at time t_2 with a new circulation n_2 and a band index λ_2 . In the following, we consider the dynamics projected onto a single Landau level, meaning that the vortex circulation is conserved ($n_1 = n_2 = n$). Formally, this corresponds to taking the limit $v_F \rightarrow +\infty$. Within a single Landau level n , the retarded Green's function takes the form¹¹

$$G_{n;\lambda_1;\lambda_2}(\mathbf{R}_1, \mathbf{R}_2) = \langle \mathbf{R}_1 | \mathbf{R}_2 \rangle e^{(l_B^2/4)\Delta_{\mathbf{R}_{12}}} [\tilde{g}_{n;\lambda_1;\lambda_2}(\mathbf{R}_{12})] \quad (12)$$

$$\mathbf{R}_{12} = \frac{1}{2} [\mathbf{R}_1 + \mathbf{R}_2 + i(\mathbf{R}_2 - \mathbf{R}_1) \times \hat{\mathbf{z}}], \quad (13)$$

where $\Delta_{\mathbf{R}}$ is the Laplacian operator. In the absence of Landau-level mixing and for a quadratic saddle-point electrostatic potential with the spatial dependence given by Eq. (1), the function \tilde{g} can be calculated exactly¹¹ with the result in the energy representation (i.e., after Fourier transformation with respect to the time difference $t_1 - t_2 = t$)

$$\tilde{g}_{n;\lambda_1;\lambda_2}(\mathbf{R}) = \int_0^{+\infty} dt \frac{-ie^{-i\tau(t)V(\mathbf{R})}}{\cosh(\sqrt{|\gamma|}t)} h_{n;\lambda_1;\lambda_2}(t) e^{it(E+i0^+)} \quad (14)$$

where $\tau(t) = (1/\sqrt{|\gamma|}) \tanh(\sqrt{|\gamma|}t)$. Here E is the energy and 0^+ an infinitesimal positive quantity. The parameters γ and ζ are geometric coefficients characterizing $V(\mathbf{r})$

$$\gamma = \frac{l_B^4}{4} [(\partial_x^2 V)(\partial_y^2 V) - (\partial_x \partial_y V)^2], \quad \zeta = \frac{l_B^2}{2} \Delta_{\mathbf{r}} V(\mathbf{r}) \quad (15)$$

The coefficient γ is directly proportional to the Gaussian curvature of the electrostatic potential, which turns out to be negative for a saddle-shaped (or hyperbolic) quadratic function $V(\mathbf{r})$. Finally, the functions $h_{n;\lambda_1;\lambda_2}(t)$, which contain the full dependences on the Landau-level index n and on the band indices λ_1 and λ_2 read for $n \geq 1$

$$h_{n;\lambda_1;\lambda_2}(t) = \sum_{\epsilon=\pm} [(1 + \epsilon\lambda_1\alpha_n)\delta_{\lambda_1,\lambda_2} + \epsilon\beta_n\delta_{-\lambda_1,\lambda_2}] \frac{e^{-itE_{n,\epsilon}}}{2}, \quad (16)$$

where $E_{n,\epsilon}$ is defined in Eq. (4),

$$\alpha_n = \frac{\sqrt{n}\hbar\Omega_c}{\sqrt{n(\hbar\Omega_c)^2 + \zeta^2/4}}, \quad \beta_n = \frac{\zeta}{\sqrt{n(\hbar\Omega_c)^2 + \zeta^2/4}} \quad (17)$$

and $h_{0;0;0}(t) = e^{-it\zeta/2}$ for the lowest Landau level $n = 0$. It is worth stressing that the previous expressions are valid for Landau-level indices n not too high, for which the inequality $|\zeta|, \sqrt{|\gamma|} \ll (\sqrt{n+1} - \sqrt{n})\hbar\Omega_c$ holds.

The action of the differential operator $\exp[(l_B^2/4)\Delta_{\mathbf{R}}]$ on the function $\tilde{g}(\mathbf{R})$ in Eq. (12) is evaluated as¹³

$$G_{n;\lambda_1;\lambda_2}(\mathbf{R}_1, \mathbf{R}_2) = \langle \mathbf{R}_1 | \mathbf{R}_2 \rangle \int \frac{d^2\mathbf{u}}{\pi l_B^2} \tilde{g}_{n;\lambda_1;\lambda_2}(\mathbf{u}) e^{-\frac{(\mathbf{u}-\mathbf{R}_{12})^2}{l_B^2}}. \quad (18)$$

Then, inserting Eq. (14) into Eq. (18), we can perform the Gaussian integrals over \mathbf{u} to get

$$G_{n;\lambda_1;\lambda_2}(\mathbf{R}_1, \mathbf{R}_2) = \langle \mathbf{R}_1 | \mathbf{R}_2 \rangle \int_0^{+\infty} dt \frac{-ie^{it(E+i0^+)}}{\cosh(\sqrt{|\gamma|}t)} h_{n;\lambda_1;\lambda_2}(t) \times \sqrt{f(t)} e^{-if(t)\tau(t)V(\mathbf{R}_{12})} e^{\gamma f(t)\tau^2(t)\frac{\mathbf{R}_{12}^2}{l_B^2}}, \quad (19)$$

with $f(t) = (1 + i\zeta\tau(t) - \gamma\tau^2(t))^{-1}$.

We note from Eq. (16) that for $n \geq 1$ and $\zeta \neq 0$ the function $h_{n;\lambda_1;\lambda_2}(t)$ is not diagonal in the λ space, indicating that λ is generically no more a good quantum number in the presence of asymmetric saddle-point potentials. A straightforward diagonalization shows that $\epsilon = \pm$ appears instead as a good number, with $h_{n;\epsilon}(t) = e^{-itE_{n,\epsilon}}$. According to the above formula (4) for $E_{n,\epsilon}$, the quantum number ϵ clearly labels the electron-like and hole-like energy bands. We shall henceforth represent the Green's function in this ϵ representation, where the latter takes a diagonal form.

In order to determine the transmission coefficient with a given energy channel (i.e., at Landau-level index n and band index ϵ fixed), we only need the Green's function $G_{n;\epsilon}(\mathbf{R}_1, \mathbf{R}_2)$ when the states at vortex positions \mathbf{R}_1 and \mathbf{R}_2 correspond to the same energy and are asymptotically far from the saddle point located at the origin. For a saddle-point potential of the form (1), this means taking the limits $|X_1| \rightarrow \infty$ and $|X_2| \rightarrow \infty$, while $V(X_1, Y_1) = V(X_2, Y_2) = \text{const.}$ Making the change in variable $s = d[1 - |\gamma|\tau^2(t)] / [1 + |\gamma|\tau^2(t)]$, where $d = |X_1 Y_2 - X_2 Y_1|/l_B^2$, we can easily take the limit $d \rightarrow +\infty$ in the integral in Eq. (19), and obtain the expression

$$G_{n;\epsilon}^{\infty}(\mathbf{R}_1, \mathbf{R}_2) = \Gamma\left(\frac{1}{2} - i\frac{E - E_{n,\epsilon}}{2\sqrt{|\gamma|}}\right) e^{-\sigma\frac{\pi}{4}\left(\frac{E - E_{n,\epsilon}}{\sqrt{|\gamma|}} + i\right)} \times (-i)e^{\frac{i(\sqrt{a}X_1 - \sqrt{b}Y_1)(\sqrt{b}X_1 + \sqrt{a}Y_1) + (\sqrt{a}X_2 + \sqrt{b}Y_2)(\sqrt{b}X_2 - \sqrt{a}Y_2)}{2l_B^2(a+b)}}} \times \frac{d^{-1/2 + i(E - E_{n,\epsilon})/(2\sqrt{|\gamma|})}}{\sqrt{4|\gamma| + 2i\zeta\sqrt{|\gamma|}}} e^{-\frac{(\sqrt{a}X_1 - \sqrt{b}Y_1)^2 + (\sqrt{a}X_2 + \sqrt{b}Y_2)^2}{2l_B^2(a+b)}}, \quad (20)$$

where $\sigma = \text{sgn}(X_1 X_2)$ and $\Gamma(z)$ is the Gamma function. At infinity the vortex is close to the asymptotes

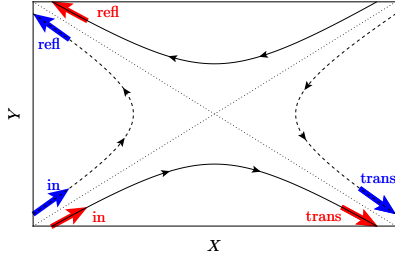


FIG. 2: (Color online) Schematic to identify the Green's functions for reflection and transmission. Semiclassically the trajectories of vortex states lie on contours of constant potential. Solid (dashed) lines correspond to an equipotential line $V > 0$ ($V < 0$) and therefore for $E > 0$ to a vortex in the conduction (valence) band, respectively. Dotted lines denote the asymptotes of the potential in Eq. (1).

of the saddle-point potential $V(\mathbf{R})$, i.e., $Y_1 \sim X_1 \sqrt{a/b}$ and $Y_2 \sim -X_2 \sqrt{a/b}$. The two modes $\epsilon = \pm$ circulate in the same direction, and are not mixed since they are well separated in energy.

Within the present saddle-point geometry, the transmission coefficient can be extracted from the asymptotic form of the retarded vortex Green's function, thus performing scattering theory in terms of coherent-state wave packets instead of the more standard plane waves. In the conduction band ($\epsilon = +$), the transmission of a vortex from the left half-plane to the right half-plane is described by Green's function expression [Eq. (20)] with the sign function $\sigma = -$ while the vortex reflection, where the vortex remains in the left half-plane, is characterized by $\sigma = +$ (see Fig. 2). Therefore, the ratio of the transmission amplitude to the reflection amplitude for a given Landau level n in the conduction band is given by the ratio of these two Green's functions:

$$\frac{t_{n,+}}{r_{n,+}} = i \exp \left[\frac{\pi}{2} \frac{E - E_{n,+}}{\sqrt{|\gamma|}} \right]. \quad (21)$$

In the valence band the vortices carry a positive charge. Therefore, the correspondence between the transmission (or reflection) process of a negative charge carrier and the sign of σ is now reversed, so that we have

$$\frac{r_{n,-}}{t_{n,-}} = i \exp \left[\frac{\pi}{2} \frac{E - E_{n,-}}{\sqrt{|\gamma|}} \right]. \quad (22)$$

The relations between the transmission probabilities $T_{n,\epsilon}$ and the transmission and reflection amplitudes, i.e., $|t_{n,\epsilon}|^2 = 1 - |r_{n,\epsilon}|^2 = T_{n,\epsilon}$, finally provide the result in Eq. (3).

For the peculiar case of the lowest Landau level, contributions both from the original conduction and valence bands arise. We get for the electron-like excitations $T_0^+(E) = \left[1 + \exp \left(-\pi(E - \zeta/2)/\sqrt{|\gamma|} \right) \right]^{-1}$, and for the hole-like excitations $T_0^-(E) = \left[1 + \exp \left(\pi(E - \zeta/2)/\sqrt{|\gamma|} \right) \right]^{-1}$. Summing up these two contributions and considering the equipartition of the current between the two types of excitations yielding a $1/2$ prefactor, we finally get the already quoted lowest Landau-level contribution

$$T_0(E) = \frac{1}{2} [T_0^+(E) + T_0^-(E)] = \frac{1}{2}. \quad (23)$$

In conclusion, we have calculated the transmission coefficient for a quadratic saddle-point electrostatic potential in graphene, and found that shape asymmetries generic to quantum point contacts break particle-hole symmetry in the conductance. Our results should be relevant for future split gate experiments in graphene as well as for the formulation of quantum network models. Theoretically, we have also presented an alternative way of deriving transmission coefficients from the scattering of coherent-state wave packets.

¹ I. Neder, N. Ofek, Y. Chung, M. Heiblum, D. Mahalu, and V. Umansky, *Nature* **448**, 333 (2007).

² H. A. Fertig and B. I. Halperin, *Phys. Rev. B* **36**, 7969 (1987).

³ J. T. Chalker and P. D. Coddington, *J. Phys. C* **21**, 2665 (1988).

⁴ B. Kramer, T. Ohtsuki, and S. Kettemann, *Phys. Rep.* **417**, 211 (2005).

⁵ This result for the 2DEG can be derived from Eqs. (1.2)-(1.6) of Ref. 2 in the limit $\omega_c \rightarrow \infty$ by neglecting the Landau-level mixing correction to the curvature energy E_1 . Such corrections lead to additional yet small contributions to the energy dependence of the transmission coefficient in the large cyclotron frequency limit, without affecting its qualitative behavior.

⁶ A. K. Geim and K. S. Novoselov, *Nature Materials* **6**, 183

(2007).

⁷ K. S. Novoselov *et al.*, *Nature* (London) **438**, 197 (2005).

⁸ Y. Zhang, Y. W. Tan, H. L. Stormer, and P. Kim, *Nature* (London) **438**, 201 (2005).

⁹ V. P. Gusynin and S. G. Sharapov, *Phys. Rev. Lett.* **95**, 146801 (2005).

¹⁰ A. H. Castro Neto, F. Guinea, N. M. R. Peres, K. S. Novoselov, and A. K. Geim, *Rev. Mod. Phys.* **81**, 109 (2009).

¹¹ T. Champel and S. Florens, *Phys. Rev. B* **82**, 045421 (2010).

¹² M. Büttiker, *Phys. Rev. B* **41**, 7906 (1990).

¹³ T. Champel and S. Florens, *Phys. Rev. B* **80**, 125322 (2009); *ibid* **80**, 161311(R) (2009).